Third A-NZ Young Geotechnical Professionals Conference, Cameron, Collingwood & Slatter (eds), Feb. 1998, Melbourne, Australia.

A Preliminary Assessment of the Behaviour of Drag Anchors in Layered Soils

M. P. O'Neill
Research Student, The University of Western Australia

Summary: This paper presents the results of a series of model drag anchor tests performed in the centrifuge on a saturated sample comprised of normally consolidated kaolin clay overlying dense silica sand. The initial focus of the paper is on the description of the test equipment and arrangement, outlining the model anchors used in the tests and the manufacture of a model instrumented anchor chain. A method of determining the orientation and embedment depth of the model anchor within the soil during each test, utilising a tracking probe attached to the anchor and "in-flight" video cameras, is also described. The results highlight the importance of the shank angle of the anchor in relation to the holding capacity and stability of the anchor/chain system.

1 INTRODUCTION

With the recent emergence of FPSO (Floating Production, Storage and Offloading) facilities as a preferred method of offshore hydrocarbon extraction, and the gradual shift of hydrocarbon discoveries towards deeper waters, greater attention has been focussed on appropriate anchoring and mooring systems. Drag embedment anchors provide a simple and economical anchoring solution, and can possess holding power to weight ratios exceeding 20.

Until recently, drag anchor design was largely empirical and based primarily on design charts developed from field test data. Furthermore, these charts describe the performance of drag anchors in homogeneous soils classified broadly as "sand" or "clay". They do not cater for drag anchor behaviour in layered soil profiles, like those encountered on the North Sea where silica sands underlie normally consolidated clays.

This paper outlines a procedure for testing model scale drag anchor and chain systems. The paper also presents the results of a number of model anchor tests using anchors with different fluke-shank angles. These tests were performed in the centrifuge in soil samples comprised of normally consolidated kaolin clay overlying dense silica sand.

2 EXPERIMENTAL DETAILS

2.1 The Centrifuge

The centrifuge at The University of Western Australia (UWA) is an Acutronic Model 661 Geotechnical Centrifuge and is rated at 40 g-tonnes, equating to a maximum payload of 200kg at an acceleration of 200 g. A swinging platform located at a radius of 1.8 m seats rectangular "strong boxes" which have internal dimensions of 650 mm long by 390 mm wide by 325 mm high, representing a prototype test bed of up to 130 m long by 80 m wide by 60 m depth. The headroom of 900 mm allows for mounting actuators which sit on top of the box and permit vertical and horizontal movements to be imposed on models.

2.2 Model Anchors and Anchor Chain

The anchor tests described in this paper were conducted using two 1:160 scale model anchors with principle dimensions similar to 32 tonne Vryhof Stevpris anchors with fluke-shank angles of 30° and 50° (Vryhof, 1990), as shown in Figure 1 (dimensions are in mm). Note that both the 30° and 50° model anchors have a fluke length of 31 mm.

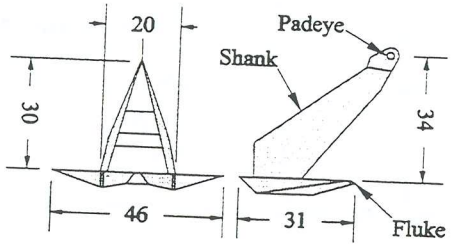

Model anchor (50° shank)

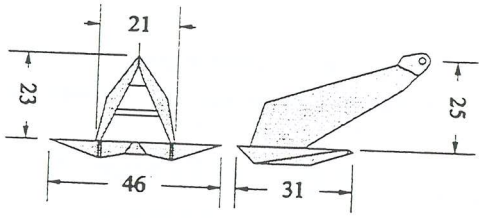

Model anchor (30° shank)

Figure 1: Model anchors

A novel model anchor chain was fabricated for the anchor tests. The chain consisted of 4 strands of 0.5 mm diameter fishing trace which were plaited in such a way as to produce a cable which has a good resemblance to a real anchor chain. The weaving of the two pairs of sinusoidal type profiles at right angles to each other results in bumps along the length of the chain which model chain links well.

In order to measure the load capacity of the model anchor as it was dragged through the test sample without disturbing the accuracy of the anchor/chain system model, a load cell was incorporated into the connection between the anchor and the chain. A miniature load cell was designed and built with four holes drilled at one end to allow attachment of the four strands of fishing trace that made up the chain. A pinned connection was located at the other end to enable the model anchor to be easily attached. The thin electrical cable from the load cell was strapped to the model chain for the first 200 mm to avoid damage to the cable.

The arrangement for each anchor test is shown in Figure 2. From the anchor, the chain is laid on the sample surface along the length of the strong box and wrapped 180 degrees around a pulley located at the end of the box. In order that the anchor chain correctly forms an inverse catenary curve from the anchor to the soil surface, where the angle of the chain with the horizontal at the surface is equal to or close to zero (Neubecker, 1995), the vertical position of the end pulley is adjustable to ensure that the chain meets the pulley at the sample surface. The chain then comes back along the length of the box and is wrapped 90 degrees around a pulley located at the base of the actuator, where it is then orientated vertically. From here the chain is wrapped 180 degrees around a third pulley located in the actuator carriage, brought back down and anchored to a padeye fixed to the actuator.

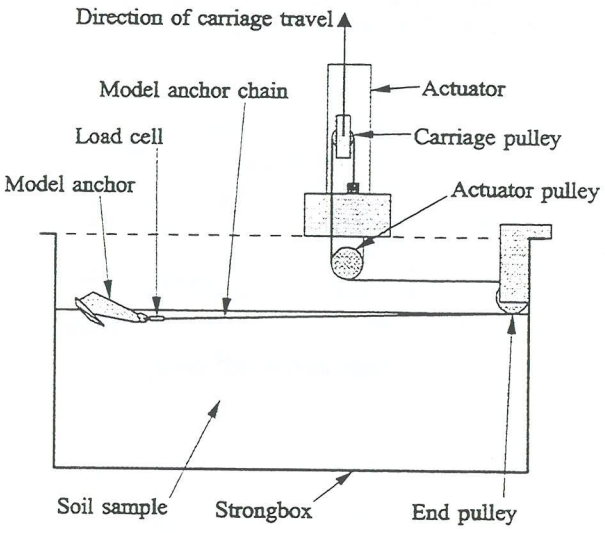

Figure 2: Testing arrangement

During an anchor test the actuator carriage is moved up, and hence there is a gearing ratio of 2:1 between the displacement of the anchor and the actuator carriage. All anchor tests presented in this paper were conducted at a carriage speed of 0.1 mm/s (corresponding to a model anchor drag speed of 0.2 mm/s).

2.3 Tracking Probe

In order to determine the position of the model anchor in the soil during the test, a tracking system developed by Neubecker (1995) was employed. A 0.6 mm steel rod was attached to the anchor just behind the padeye, as shown in Figure 3. A board consisting of two parallel black and white scales 50 mm apart was mounted horizontally and directly above the line of travel of the anchor padeye. The probe was approximately 160 mm in length to ensure that it protruded a significant distance from the soil. Hence, during the test the tracking probe would travel close to the horizontal scales, allowing the orientation and drag distance of the anchor to be determined. The tracking probe was also marked with a black and white scale to indicate distance from the anchor padeye, and enabled the embedment depth of the anchor padeye to be calculated.

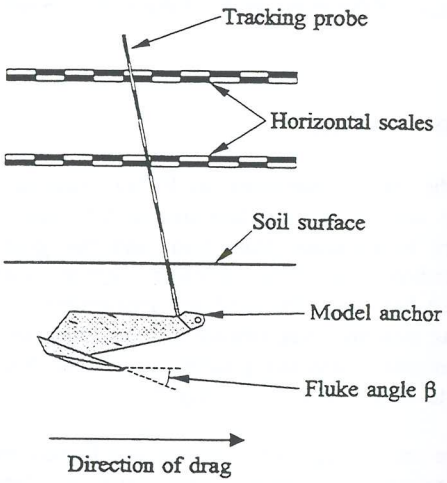

Figure 3: Tracking probe

Two video cameras were mounted on top of the strong box at approximately the same level as the horizontal scales to enable observation of the tracking probe as it moved past the scales. The signals from both cameras were recorded on video tape to allow a detailed analysis of the movement of the anchor to be conducted after the test. The scope of each video camera was such that only about half of the full drag length of each test could be observed before the tracking probe went out of range. Hence, the cameras were carefully positioned to ensure that the probe was always within the viewing range of one of the cameras, and that there was an overlap in the views of both cameras as the probe moved from the range of one camera to the other.

After each test the movement of the tracking probe past the scales was digitised. This involved the use of a frame-grabbing computer to save an image from the recorded video signals as an image file every 30 seconds during the test. The saved images were then put into a graphics program. Two points along the length of the tracking probe which were within view of the cameras during the entire test were

selected. Each image was analysed separately to allow the x-z coordinates of the selected points to be determined. Additional information from each image was also gathered in order to correct for parallax effects. The data from all images was then syncronised with the data obtained from the anchor chain load cell.

2.4 Sample Preparation

The anchor tests described in this paper were conducted in a fully saturated sample comprised of dense silica sand underlying normally consolidated kaolin clay. The depth of the clay layer for the first two tests was 14 mm (2.2 m at prototype scale), while for the last two tests it was 35 mm (5.6 m at prototype scale).

Initially, a fine mesh and a thin layer of coarse sand was placed over a drainage hole at the base of the strong box. In order that the silica sand layer possess as high a density as possible, the silica sand was placed dry into the strong box by slow raining using an automatic sand rainer. At the conclusion of the raining, the sand surface was vacuum levelled to the required height of 185 mm. The strong box was then weighed in order to determine the density of the sand, which came out to be 16.7 kN/m^3. This compares reasonably well with the maximum dry density of 17.0 kN/m^3 (Neubecker, 1995).

The sand sample was then saturated by slow upwards percolation of water through the base drainage hole. Saturation was continued until there was at least 50 mm of water above the sand surface.

The kaolin clay was prepared as a slurry which was mixed under a vacuum for several hours to de-air the soil. The slurry was then carefully placed in the strong box over the silica sand to the required height, ensuring that no air was trapped in the slurry and that the surface of the sand was not disturbed. A miniature pore pressure transducer was placed within the clay slurry to allow measurement of the dissipation of pore pressure during consolidation in the centrifuge.

The strong box was placed in the centrifuge, where the sample underwent a slow consolidation procedure designed to minimise infiltration of the clay layer into the sand. This process involved a gradual ramp-up at acceleration levels of 10 g, 20 g, 40 g and 80 g before reaching the target acceleration level of 160 g. At each level, the sample was allowed to consolidate until the pore pressure reached a plateau.

At the conclusion of the second anchor test (Test 7.3), additional de-aired kaolin slurry was added to the test sample, and the sample allowed to reconsolidate at the full target acceleration of 160 g.

3 EXPERIMENTAL RESULTS

3.1 Sample Details

Four anchor tests using the 30° and 50° model anchors were conducted in the test sample, covering two different normally consolidated clay layer depths as shown in Table 1. Each test was adequately spaced along the width of the strong box to avoid clashing of the failure zones of soil.

Test Number	Anchor Type	Clay Depth (m)
7.1	50° shank	2.2
7.3	30° shank	2.2
7.4	30° shank	5.6
7.5	50° shank	5.6

Table 1: Anchor test summary

Prior to Tests 7.1 and 7.4, cone penetration tests (CPT 1 and CPT 2 respectively) were conducted in order to determine the friction angle of the test sample. The method for its calculation was proposed by Robertson and Campanella (1983), and involves an empirical correlation between the bearing capacity factor, N_q, and the friction angle, ϕ'. Figure 4 shows the cone resistance profiles obtained from both cone tests, which indicated a friction angle of approximately 42°.

Prior to Test 7.4 and in addition to the cone test (CPT 2), the undrained shear strength (s_u) profile of the 5.6 m normally consolidated clay layer was determined using a t-bar apparatus (Stewart and Randolph, 1991). As indicated in Figure 4 (T-bar 1), the shear strength gradient was approximately 1.1 kPa/m. No t-bar test was performed prior to Test 7.1 because the clay layer was relatively shallow (14 mm at model scale), making it difficult to gather any strength data. However, it is reasonable to assume that the undrained shear strength gradient of the 2.2 m clay layer was also approximately 1.1 kPa/m.

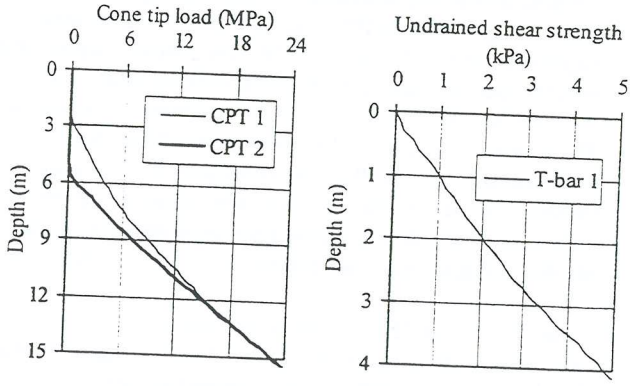

Figure 4: Cone penetrometer and t-bar tests

3.2 Anchor Tests

Figure 5 shows the plots of anchor capacity against horizontal padeye displacement (in fluke lengths) for Tests 7.1 and 7.3 (using the 50° and 30° anchors respectively). The anchor capacity is expressed in terms of anchor efficiency, which is the ratio of the holding power of the anchor to the anchor dry weight. Note that displacement data was gathered at 30 second intervals, and therefore the curves appear stepwise in nature. Both tests show a steady increase in capacity in the first fluke length of drag. By 2 fluke lengths the capacity

developed by the 50° anchor had leveled out at an efficiency of approximately 6.7, and remained at that level for the rest of the drag. The capacity of the 30° anchor peaked at an efficiency of 9.4 at 2 fluke lengths of drag, before dropping slightly to 7.5 at 5 fluke lengths. This capacity was maintained until the conclusion of the test.

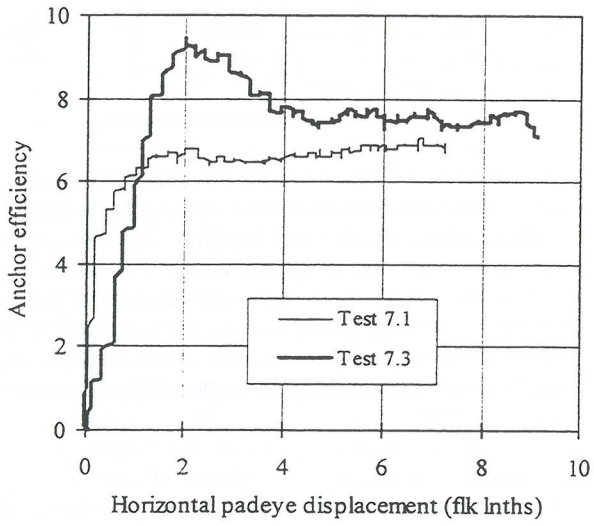

Figure 5: Anchor efficiency vs horizontal padeye displacement - Tests 7.1 and 7.3

Similar efficiency curves plotted against horizontal padeye displacement for Tests 7.4 and 7.5 are shown in Figure 6. The capacity of the 50° anchor (Test 7.5) leveled out at an efficiency of approximately 8.6 after a drag length of 2 fluke lengths, and then proceeded to decrease slightly over the rest of the drag to an efficiency of 7.6. The 30° anchor peaked at an efficiency of 12.4 after a little over 2 fluke lengths of drag, before steadily dropping to 9.8 at 8 fluke lengths.

The results show that the capacities of the anchors were significantly higher in the tests conducted in the sample with a deeper clay layer. Furthermore, the capacity of the anchor with the 30° shank was markedly higher than the anchor with the 50° shank in both clay depths.

Figure 7 shows the anchor fluke angle β plotted against horizontal padeye displacement for Tests 7.1 and 7.3, where β is measured as the angle of the upper surface of the anchor flukes to the horizontal (Figure 3). Prior to dragging in both tests, the anchor was orientated with the front tips of the flukes and the anchor padeye approximately level (β values of 80° and 58° for the 50° and 30° anchors respectively). At the commencement of dragging, both anchors began to rotate with the fluke angle β decreasing. However, within the first half a fluke length of drag, the rate of rotation of the 50° anchor dropped substantially, and by 2 fluke lengths of drag had ceased rotating altogether at a fluke angle of 66°. On a number of occasions during the rest of the drag, the 50° anchor rotated backwards slightly (β increase) before re-orientating itself back to a fluke angle of around 65°.

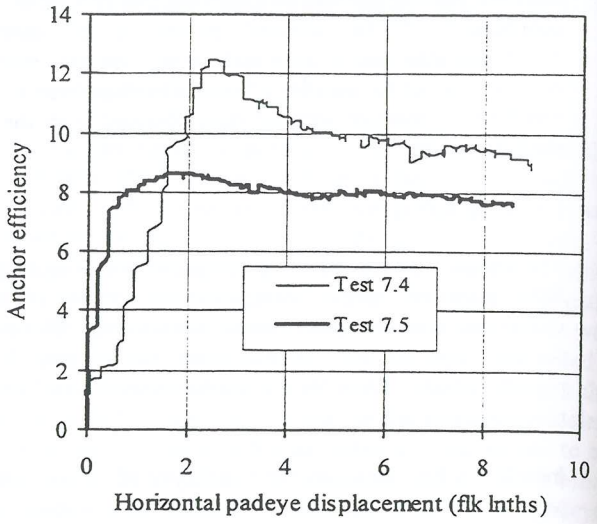

Figure 6: Anchor efficiency vs horizontal padeye displacement - Tests 7.4 and 7.5

Unlike the 50° anchor, the 30° anchor continued to rotate with β decreasing at a steady rate down to a value of 22° at 2 fluke lengths of drag, then decreasing further but at a slower rate to a value of 12° at 9 fluke lengths of drag. Note that the point of change in the rate of rotation corresponds approximately with the maximum anchor capacity measured (Figure 5).

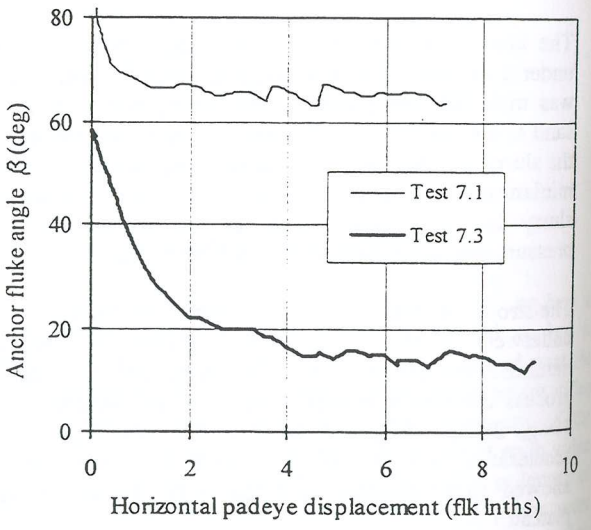

Figure 7: Anchor fluke angle β vs horizontal padeye displacement - Tests 7.1 and 7.3

The curves showing the fluke angle β of the model anchors during the drags in the sample comprised of the deeper clay layer (Tests 7.4 and 7.5) are featured in Figure 8. The small gap in the curve for Test 7.4 is the result of unclear video images and the inability to obtain accurate x-z coordinates from these images. As with Tests 7.1 and 7.3, these drags commenced at relatively high fluke angles. Both anchors rotated with β reducing in the early stages of each test. The

rotation rate of the 50° anchor (Test 7.5) reduced significantly at approximately half a fluke length of drag, but unlike Test 7.3 which was conducted in a shallower clay layer, the anchor continued to rotate, with the fluke angle reaching 51° after 8 fluke lengths of drag. In Test 7.4, the anchor rotated to a lower β value of 16° after 3 fluke lengths, and remained at 16° to 22° for the rest of the test.

In both 30° anchor tests, a relatively low fluke angle was reached and maintained, accompanied by good development of holding capacity. For the case of the 50° anchor tests, less rotation was observed, and on occasion the anchor rotated back to a higher fluke angle, suggesting that the anchor was attempting to "dig" into the sand but became unstable when β became too low.

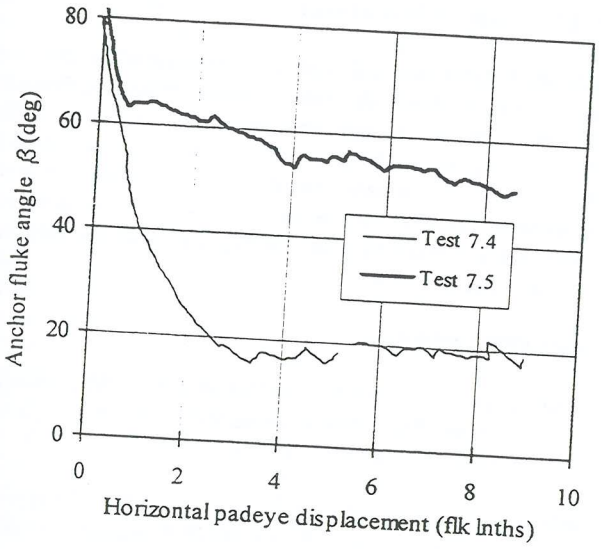

Figure 8: Anchor fluke angle β vs horizontal padeye displacement - Tests 7.4 and 7.5

The embedment depths of both the anchor padeye and the front fluke tips plotted against horizontal padeye displacement for Tests 7.1 and 7.3 are shown in Figure 9. For these tests, the sand/clay interface was at a depth of 2.2 m (prototype scale) or 0.45 fluke lengths. At the commencement of each test, the anchor padeye and fluke tips were at approximately the same level. In both tests the anchor padeye reached the sand/clay interface within the first 2 fluke lengths of drag, but upon further dragging did not penetrate into the sand layer.

The fluke tips in Test 7.1 (50° anchor) penetrated partially into the sand, reaching a depth of 0.60 fluke lengths (or 0.15 fluke lengths into the sand) at a little under 2 fluke lengths of drag. However, as the anchor ceased to rotate (Figure 7) the depth of the fluke tips within the sample quickly decreased back to approximately 0.54 fluke lengths, just below the sand/clay interface. Again, the fluke tips were attempting to dig into the sand, but this quickly caused the anchor to become unstable. Upon further dragging, the fluke tips continually embedded and pulled out of the sand, unable to embed deeper than 0.70 fluke lengths into the sample (0.25 fluke lengths into the sand layer). In Test 7.3 (30° anchor), the fluke tips reached a sample depth of 1.00 fluke length (0.55 fluke lengths into the sand) within the first 2 fluke lengths of drag. Further embedment of the fluke tips was observed during the remainder of the test (up to 1.1 fluke lengths), and was due mainly to small rotations of the anchor.

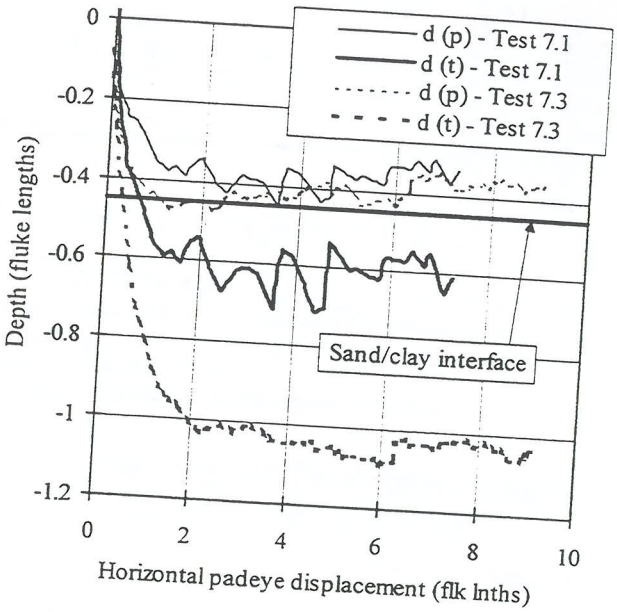

Figure 9: Padeye (p) and fluke tip (t) depth vs horizontal padeye displacement - Tests 7.1 and 7.3

The anchor padeye and fluke tip embedment plots for Tests 7.4 and 7.5 are shown in Figure 10. In these tests, the sand/clay interface was located at a depth of 5.6 m (prototype scale) or 1.13 fluke lengths. As before, the anchor padeye in both tests quickly reached the interface, but did not penetrate into the sand in any significant way during further dragging. The fluke tips of the 30° anchor (Test 7.4) again showed reasonable embedment, reaching a maximum depth of 1.74 fluke lengths (0.61 fluke lengths into the sand layer) within a little over 2 fluke lengths of drag. Despite a minor reduction in embedment depth at around 4.4 fluke lengths of drag the fluke tips remained relatively stable at a depth of approximately 1.65 fluke lengths for the remainder of the test.

Unlike Test 7.1, where the fluke tips of the 50° anchor made no significant penetration into the sand layer, in Test 7.5 the tips embedded at a steady rate to approximately 1.55 fluke lengths (0.51 fluke lengths into the sand) after 4 fluke lengths of drag. The tips then remained at an embedment depth of 1.50 fluke lengths for a further 2 fluke lengths of drag. Towards the end of the test, the tips were observed to increase in depth, reaching 1.70 fluke lengths at the conclusion of dragging. It would have been interesting if the drag could have proceeded a further few fluke lengths, in order to determine whether the tips would have embedded further, whether the anchor had reached a point of stability or whether the anchor was on the verge of pulling out.

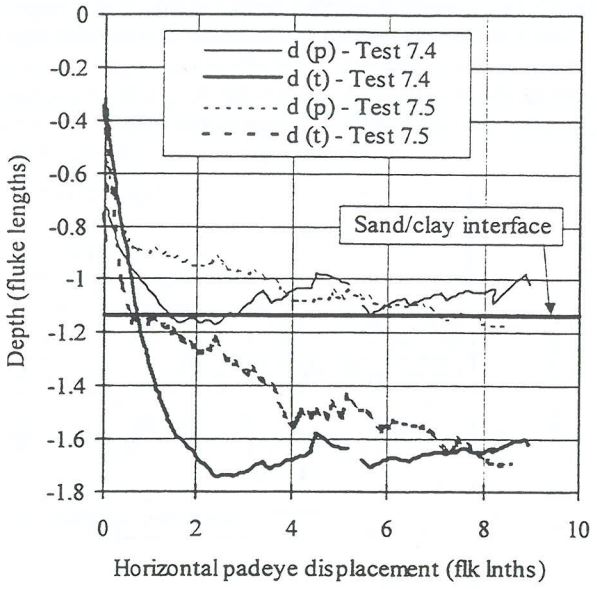

Figure 10: Padeye (p) and fluke tip (t) depth vs horizontal padeye displacement - Tests 7.4 and 7.5

4 CONCLUSIONS

Results have been presented from a series of model drag anchor and anchor chain tests performed in the centrifuge at The University of Western Australia in saturated samples comprised of a thin layer of normally consolidated clay overlying dense silica sand.

By incorporating a miniature load cell into the anchor chain without disturbing the accuracy of the anchor/chain system, and by employing a tracking system in order to determine the orientation and embedment of the model anchor during testing, a comprehensive description of both the development of anchor holding power and the anchor kinematics was obtained.

The model anchor with the 30° shank was able to rotate to shallower fluke angles and embed further than the anchor with the 50° shank. This in turn led to the 30° anchor generating higher holding capacities and remaining more stable with continued dragging.

In many instances, the experimental data showed the anchor continually digging into the sand layer, becom unstable and partially pulling out. This result was expec since the 30° anchor is used predominantly in sand, while 50° anchor is used in softer soils. Interestingly, experimental data showed that in those tests where the fl tips did embed into the sand, only minimal embedment of shank into the sand was achieved.

Further tests will be conducted covering a wider range of c layer depths and soil conditions. The results, together with anchor theory developed by Neubecker (1995), will be used develop a simulation program to predict drag anch embedment and capacity in layered cohesive and n cohesive soils

5 ACKNOWLEDGEMENTS

The work described in this paper forms part of the activities the Special Research Centre for Offshore Foundati Systems, funded through the Australian Research Counci Research Centre's Program. The author is supported by University Postgraduate Award. Special thanks are due to t workshop and centrifuge staff at UWA, without who excellent technical support the experimental research wou not have been possible.

6 REFERENCES

Neubecker, S. R. (1995), The behaviour of drag anchor a chain systems, PhD Thesis, Department of Civil Engineerin The University of Western Australia.

Robertson, P. K. and Campanella, R. G. (1983), Interpretatio of cone penetration tests. Part 1: Sand. Canadian Geotechnic Journal, 20, 718-733.

Stewart, D. P. and Randolph, M. F. (1991), A new sit investigation tool for the centrifuge, *Centrifuge 91*, Balkema Rotterdam, pp531-538.

Vryhof Anchors. 1990. *Anchor Manual*. Krimpen ad Ysse The Netherlands.